

1959

Analysis of Creep in Rotating Hollow Disks Based on the Maximum Shear Theory

Philip Lung-Mao Ko

Follow this and additional works at: <https://openprairie.sdstate.edu/etd>

Recommended Citation

Ko, Philip Lung-Mao, "Analysis of Creep in Rotating Hollow Disks Based on the Maximum Shear Theory" (1959). *Electronic Theses and Dissertations*. 2582.
<https://openprairie.sdstate.edu/etd/2582>

This Thesis - Open Access is brought to you for free and open access by Open PRAIRIE: Open Public Research Access Institutional Repository and Information Exchange. It has been accepted for inclusion in Electronic Theses and Dissertations by an authorized administrator of Open PRAIRIE: Open Public Research Access Institutional Repository and Information Exchange. For more information, please contact michael.biondo@sdstate.edu.

ANALYSIS OF CREEP IN ROTATING HOLLOW DISKS

BASED ON THE MAXIMUM SHEAR THEORY

BY

PHILIP LUNG-MAO KO

A thesis submitted
in partial fulfillment of the requirements for the
degree Master of Science, Department of
Mechanical Engineering, South Dakota
State College of Agriculture
and Mechanic Arts

August, 1959

SOUTH DAKOTA STATE COLLEGE LIBRARY

ANALYSIS OF CREEP IN ROTATING HOLLOW DISKS

BASED ON THE MAXIMUM SHEAR THEORY

This thesis is approved as a creditable, independent investigation by a candidate for the degree, Master of Science, and acceptable as meeting the thesis requirements for this degree; but without implying that the conclusions reached by the candidate are necessarily the conclusions of the major department.

Thesis Adviser

Head of the Major Department

ACKNOWLEDGMENTS

The author wishes to express his sincere appreciation to Professor Benjamin Ma of the Mechanical Engineering Department for his helpful suggestions, criticisms, and guidance throughout this study and in preparation of the manuscript.

Appreciation is also expressed to staff members of the General Engineering Department for their cooperation and assistance, and to Mrs. Joyce Furubotten for her patience and time devoted to the typing of this thesis.

PLK

TABLE OF CONTENTS

	Page
INTRODUCTION	1
NOMENCLATURE	3
ANALYSIS OF CREEP	5
GENERAL EQUATIONS FOR CREEP RATES AND DEFORMATIONS	8
CREEP ANALYSIS IN ROTATING HOLLOW DISKS	12
Case I. Constant Thickness and Constant Temperature Hollow Disk Under Steady-State Conditions	14
Case II. Variable Thickness and Constant Temperature Hollow Disk Under Steady-State Conditions	22
NUMERICAL EXAMPLE OF A ROTATING HOLLOW DISK	29
Elastic Stresses	29
Creep Stresses	31
SUMMARY AND CONCLUSIONS	45
LITERATURE CITED	48

LIST OF TABLES

Table		Page
I.	CALCULATION OF RADIAL STRESSES IN ROTATING HOLLOW DISK OF VARIABLE THICKNESS FOR ELASTIC CONDITION	32
II.	CALCULATION OF TANGENTIAL STRESSES IN ROTATING HOLLOW DISK OF VARIABLE THICKNESS FOR ELASTIC CONDITION	33
III.	CALCULATION OF FIRST APPROXIMATION FOR STRESSES IN ROTATING HOLLOW DISK OF VARIABLE THICKNESS	36
IV.	CALCULATION OF SECOND APPROXIMATION FOR STRESSES IN ROTATING HOLLOW DISK OF VARIABLE THICKNESS	37
V.	CALCULATION OF THIRD APPROXIMATION FOR STRESSES IN ROTATING HOLLOW DISK OF VARIABLE THICKNESS	38
VI.	CALCULATION OF RELATIVE CREEP RATES BASED ON THE THIRD APPROXIMATION OF THE STRESSES IN ROTATING HOLLOW DISK OF VARIABLE THICKNESS	39

LIST OF FIGURES

Figure	Page
1. Variation of Creep Curves (a) with Stress ($s_3 > s_2 > s_1$) and (b) with Temperature ($T_3 > T_2 > T_1$)	5
2. Creep Strain - Time Relation	6
3. Constant - Thickness Rotating Hollow Disk	15
4. Variable - Thickness Rotating Hollow Disk	23
5. The Stress Distribution of the Disk for Elastic Condition	40
6. The Stress Distributions of the Disk Under Creep Conditions for $n=6$	41
7. Comparison of Stress Distribution in the Disk Under Elastic and Creep Conditions	43
8. The Relative Creep Rates of the Disk (Based on Third Approximation of the Stresses)	44

INTRODUCTION

With the advent of gas turbines and jet engines, the rotating disks are generally required to operate under high speeds and elevated temperatures frequently exceeding the yield strength of the materials currently available and resulting in plastic flow. The stress distribution in rotating disks under these conditions cannot be properly estimated on the basis of the theory of elasticity. In addition to this, the creep deformations of rotating disks with time must also be determined in order to maintain adequate clearances between turbine blades and shrouds.

The problem of creep deformations and stress distributions in rotating disks operating at high temperature has been under active consideration for many years. Although a great many theoretical investigations of rotating disks have been reported in the technical literature, most of these consider only elastic deformations and stresses. Only a very few deal with the theoretical calculation of creep stresses in rotating disks that operate for long periods at elevated temperatures.

Several investigators, among them such as Bailey¹, Soderberg²,

¹R. W. Bailey, "The Utilization of Creep Test Data in Engineering Design," Proc. Institution of Mechanical Engineers, vol. 131, 131-349, Institute of Mechanical Engineers: London, November, 1935.

²C. R. Soderberg, "The Interpretation of Creep Tests for Machine Design," Trans. ASME, vol. 58, 733-743, The American Society of Mechanical Engineers: New York, 1936.

Popov³, Millenson and Manson⁴, and Johnson⁵, proposed formulas for calculating stress distributions in rotating disks under creep conditions. They considered the creep as a function of distortion strain energy. These formulations are fundamentally alike and are essentially extensions of the theory of plastic flow in crystalline materials.⁶ However, it was found that these methods of calculating stress distributions and creep deformations in rotating disks gave creep deformations much too low, on the unsafe side for design, compared to the average test values.

This paper presents an analysis of creep in rotating disks that operate at elevated temperatures. This analysis of creep is based on the maximum shear theory instead of the distortion energy theory or the Mises criterion. The results show a considerable simplification in the analysis and good agreement with the average test data of rotating disks⁷. Only hollow disks are discussed in this paper.

³E. P. Popov, "Stresses in Turbine Disks at High Temperatures," Journal of the Franklin Institute, vol. 243, 365-389, Franklin Institute: Philadelphia, Pennsylvania, 1947.

⁴M. B. Millenson and S. S. Manson, "Determination of Stresses in Gas-Turbine Disks Subjected to Plastic Flow and Creep," NACA Report, No. 906, National Advisory Committee for Aeronautics: Washington, D. C., 1948.

⁵A. E. Johnson, "Turbine Disks for Jet Propulsion Units," Aircraft Engineering, pp. 265-272, Aircraft Engineering: England, August, 1956.

⁶A. Nadai, Plasticity, Engineering Societies Monographs, McGraw-Hill: New York, 1931.

⁷A. M. Wahl, G. O. Sankey, M. J. Manjoine, and E. Shoemaker, "Creep Tests of Rotating Disks at Elevated Temperature and Comparison with Theory," Trans. ASME, vol. 76, 225-235, The American Society of Mechanical Engineers: New York, 1954.

NOMENCLATURE

The following nomenclature is used in the paper:

A	radial cross-sectional area of disk
A_r	radial cross-sectional area of disk from r_1 to r
a, b, K, k	constants
h, h_1, h_0	thickness of disk at radii r, r_1, r_0
I	moment of inertia of disk
I_r	moment of inertia of disk from r_1 to r
n	material creep number
r	radius to any point of disk
r_1, r_0	inner and outer radii of hollow disk
T	temperature
t	time
w	radial deformation of disk at radius r
\dot{w}, \dot{w}_1	radial deformation rates at radii r, r_1
x	stress ratio
$\dot{\epsilon}$	effective creep rate
$\dot{\epsilon}_1, \dot{\epsilon}_2, \dot{\epsilon}_3$	principal creep rates
$\dot{\epsilon}_r, \dot{\epsilon}_t, \dot{\epsilon}_z$	radial, tangential, axial creep rates of disk
$\epsilon_1, \epsilon_2, \epsilon_3$	principal creep strains
$\epsilon_r, \epsilon_t, \epsilon_z$	radial, tangential, axial creep strains of disk
$\epsilon_{r_1}, \epsilon_{r_0}$	tangential creep strains of disk at radii r_1, r_0
ρ	density of disk
σ	effective stress

- $\sigma_1, \sigma_2, \sigma_3$ principal stresses
- $\sigma_r, \sigma_t, \sigma_z$ radial, tangential, axial stresses of disk
- $\sigma_{r_1}, \sigma_{r_0}$ radial stresses of disk at radii r_1 and r_0
- σ_{tav} average tangential stress of disk
- $\sigma_{t_1}, \sigma_{t_0}$ tangential stresses of disk at radii r_1 and r_0
- ϕ flow function
- ω angular velocity
- ν Poisson's ratio

ANALYSIS OF CREEP

Creep is frequently defined as the continuous deformational responses to constant stress of material over a long time at a moderately high temperature. This definition, however, is too narrow to cover all aspects of the phenomenon of creep because of its complicated nature. The complexity of the phenomenon of creep is not only due to the interaction of the constituent phases of material during the deformation, but also due to the difference in the responses of those phases to changes of parameters of the test, that is, the changes of stress, time, and temperature. The general creep-strain-time relations with stress and with temperature are shown schematically in Figure 1.

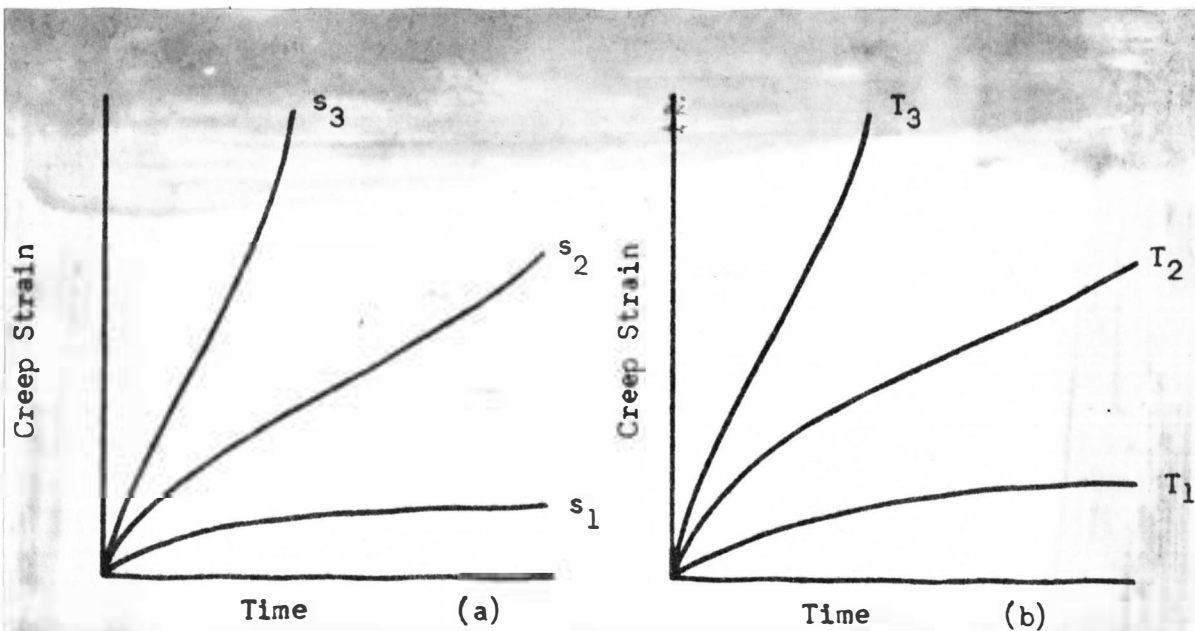


Figure 1. Variation of Creep Curves (a) with Stress ($s_3 > s_2 > s_1$) and (b) with Temperature ($T_3 > T_2 > T_1$)

In this paper, the phases of metallographical transformations at high temperatures will not be considered. The stress analysis presented applies only to materials found stable for high temperature service. Furthermore, the analysis is primarily confined to creep deformations and stresses that occur during the steady state as shown in Figure 2.

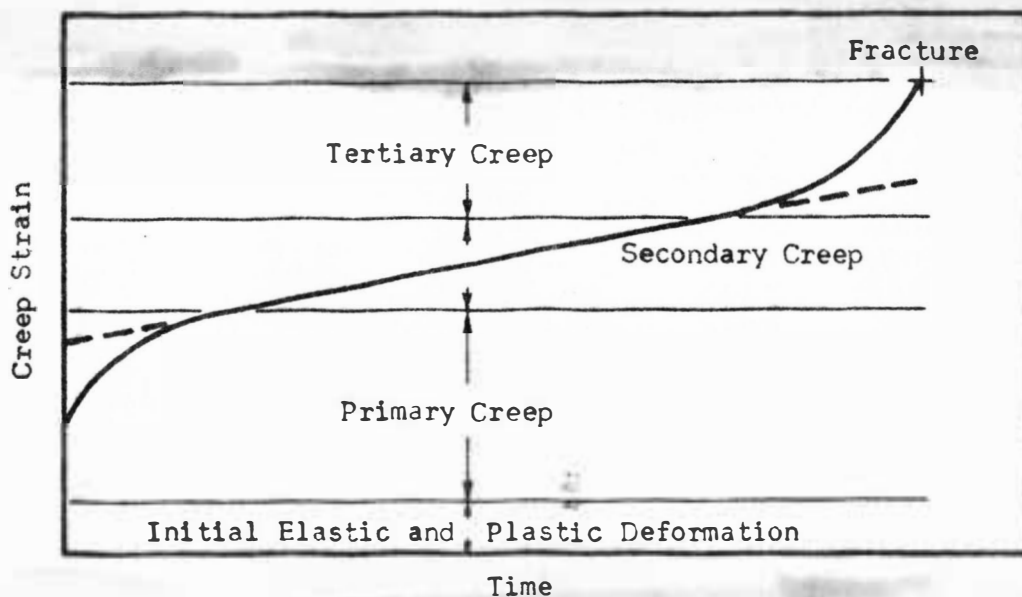


Figure 2. Creep Strain - Time Relation

In making the analysis of creep deformations for the rotating disks at elevated temperatures under steady-state conditions, the following postulates are made:⁸

1. The directions of the principal strains coincide with those

⁸A. Nadai, Theory of Flow and Fracture of Solids, Monographs, McGraw-Hill: New York, 1950.

of the principal stresses at all times.

2. The density or the volume of the material remains unchanged.
3. The principal shear strains are proportional to the principal shear stresses.

Besides these postulates for creep, five additional assumptions are introduced:

1. The relatively small elastic deformations for the disks may be neglected in comparison with large deformations due to creep.
2. The axial stress may be neglected and the radial and tangential stresses are uniform across the thickness of the disk.
3. All variables of material properties and operating conditions are symmetrical about the axis of rotation.
4. The yield condition follows the maximum shear theory in which the maximum shearing stress is the determining factor affecting the creep of the material.
5. For the steady state of creep, the simplest and most widely used power creep law is satisfactory.

GENERAL EQUATIONS FOR CREEP RATES AND DEFORMATIONS

For predicting the creep rates, evidently the time must be considered as a new additional independent variable. This is true for all metals at sufficiently high temperatures. For a given material, the creep rate at which the creep deformation changes with respect to the time at a constant stress increases very rapidly with increasing temperatures. The similar situation occurs for a given material at a constant temperature with increasing stresses. The creep rate, therefore, may be considered as a function of stress, time, and temperature.

Then we may further assume that

$$\dot{\epsilon} = F(\sigma) f(t) g(T) \quad (1)$$

on the basis of creep test results.

From the assumption 5, however, the function of stress may be expressed in the following form

$$F(\sigma) = K \sigma^n$$

where K and n are constants.

Because of the complexity of the creep problem, the temperature gradients in the disks will not be discussed here.

Therefore, from the preceding discussion, Equation (1) of the creep rate may be rewritten as

$$\dot{\epsilon} = K \sigma^n f(t) g(T) \quad (2)$$

It is realized that Equation (2) of the creep rate does not always hold true^{9, 10, 11, 12}, however, in many cases creep data obtained under essentially constant stress may be represented with sufficient approximation for engineering work in this manner. No attempt is made here to justify the use of this equation for all materials. It is used here because it results in rather simple expressions for stress in certain cases.

According to the assumptions of stationary or steady plastic flow, the principal strain rates $\dot{\epsilon}_1, \dot{\epsilon}_2, \dot{\epsilon}_3$ are given in the following form by¹³

$$\begin{aligned}\dot{\epsilon}_1 &= \phi \left[\sigma_1 - \frac{\sigma_2 + \sigma_3}{2} \right] \\ \dot{\epsilon}_2 &= \phi \left[\sigma_2 - \frac{\sigma_3 + \sigma_1}{2} \right] \\ \dot{\epsilon}_3 &= \phi \left[\sigma_3 - \frac{\sigma_1 + \sigma_2}{2} \right]\end{aligned}\tag{3}$$

⁹R. W. Bailey, "Creep Relationships and Their Application to Pipes, Tubes, and Cylindrical Parts Under Internal Pressure," Proc. Institution of Mechanical Engineers, vol. 164, 425, Institute of Mechanical Engineers: London, 1951.

¹⁰A. E. Johnson, "Creep Under Complex Stress Systems at Elevated Temperatures," Proc. Institution of Mechanical Engineers, vol. 164, 433, Institute of Mechanical Engineers: London, 1951.

¹¹F. K. G. Odquist, "Recent Advances in Theories of Creep of Engineering Materials," Applied Mechanics Reviews, vol. 7, 517, The American Society of Mechanical Engineers: New York, 1954.

¹²O. D. Sherby and J. E. Dorn, "An Analysis of the Phenomenon of High Temperature Creep," Proc. Society for Experimental Stress Analysis, vol. XII, No. 1, pp. 139-153, Society for Experimental Stress Analysis: Cambridge, Massachusetts, 1954.

¹³Nadai, Theory of Flow and Fracture of Solids, op. cit.

in which ϕ is a quantity to be determined.

Assuming that the principal stresses are in the order $\sigma_1 > \sigma_2 > \sigma_3$, from the maximum shear theory, it can be expressed as

$$\sigma_1 - \sigma_3 = \sigma$$

where σ is the yield stress in tension and is also called the effective stress.

Then, from Equation (3), we may have the effective creep rate

$$\begin{aligned} \dot{\epsilon} &= \dot{\epsilon}_1 - \dot{\epsilon}_3 \\ &= \phi \left[\sigma_1 - \frac{\sigma_2 + \sigma_3}{2} \right] - \phi \left[\sigma_3 - \frac{\sigma_1 + \sigma_2}{2} \right] \end{aligned}$$

or in the simpler form

$$\dot{\epsilon} = \frac{3}{2} \phi [\sigma_1 - \sigma_3] = \frac{3}{2} \phi \sigma \quad (4)$$

Setting the right hand terms of Equations (2) and (4) equal to each other, and solving for the undetermined quantity ϕ , one has

$$\phi = \frac{2}{3} K \sigma^{n-1} f(t) g(T)$$

or

$$\phi = k \sigma^{n-1} f(t) g(T) \quad (5)$$

where k is equal to $\frac{2}{3} K$ and is a constant which can be determined from the creep tests.

Substituting Equation (5) into Equations (3), the general equations for the creep strain rates under steady state conditions are obtained as follows:

$$\dot{\epsilon}_1 = \kappa \sigma^n \left[\frac{2\sigma_1 - \sigma_2 - \sigma_3}{2\sigma} \right] f(t) g(T)$$

$$\dot{\epsilon}_2 = \kappa \sigma^n \left[\frac{2\sigma_2 - \sigma_1 - \sigma_3}{2\sigma} \right] f(t) g(T) \quad (6)$$

$$\dot{\epsilon}_3 = \kappa \sigma^n \left[\frac{2\sigma_3 - \sigma_1 - \sigma_2}{2\sigma} \right] f(t) g(T)$$

CREEP ANALYSIS IN ROTATING HOLLOW DISKS

The following rotating-hollow-disk cases are analyzed by using the maximum-shear theory with the flow rule associated with the distortion energy theory or the Mises criterion. It is considered that the disk has a central hole with diameter slightly greater than its thickness, and that the axial stresses vanish throughout the disk.

Case I. Constant thickness and constant temperature disk under steady state conditions.

Case II. Variable thickness and constant temperature disk under steady state conditions.

Under steady state conditions, the principal creep strains are equal to steady or minimum creep rates multiplied by time, or may be written as follows:

$$\begin{aligned}\epsilon_1 &= \int_0^t \dot{\epsilon}_1 dt \\ \epsilon_2 &= \int_0^t \dot{\epsilon}_2 dt \\ \epsilon_3 &= \int_0^t \dot{\epsilon}_3 dt\end{aligned}\tag{7}$$

Now if we let \dot{w} be the rate of steady change with time of the radial deformation, then the radial deformation during the steady state is equal to the radial deformation rate multiplied by time, that is

$$w = \int_0^t \dot{w} dt$$

From this it follows that the tangential and the radial creep strains are

$$\epsilon_1 = \int_0^t \left(\frac{\dot{w}}{r} \right) dt$$

and

$$\epsilon_2 = \int_0^t \left(\frac{d\dot{w}}{dr} \right) dt, \text{ respectively.}$$

But by comparing these with Equations (7), we may express the steady creep rates for the tangential and the radial directions as

$$\dot{\epsilon}_1 = \frac{\dot{w}}{r}$$

and

$$\dot{\epsilon}_2 = \frac{d\dot{w}}{dr}, \text{ respectively.}$$

In our case of the thin rotating disk, the axial stress vanishes, that is, $\sigma_3 = 0$. So by writing Equations (6) with only the two principal stresses, one obtains

$$\dot{\epsilon}_1 = \frac{\dot{w}}{r} = k \sigma^n \left[\frac{2\sigma_1 - \sigma_2}{2\sigma} \right] f(t) g(T) \quad (8)$$

$$\dot{\epsilon}_2 = \frac{d\dot{w}}{dr} = k \sigma^n \left[\frac{2\sigma_2 - \sigma_1}{2\sigma} \right] f(t) g(T)$$

From the assumption 2 in the plastic flow theory, the condition of incompressibility of the material furnishes the following relations:

$$\epsilon_1 + \epsilon_2 + \epsilon_3 = 0$$

or

$$\dot{\epsilon}_1 + \dot{\epsilon}_2 + \dot{\epsilon}_3 = 0 \quad (9)$$

Since the effective stress σ is based on the maximum shear theory and in the case of the rotating disk, we considered $\sigma_t > \sigma_r > \sigma_z = 0$, in which $\sigma_t = \sigma_1$, $\sigma_r = \sigma_2$ and $\sigma_z = \sigma_3$, the minimum principal stress

σ_3 is zero and hence σ may be taken as σ_1 , in Equations (8).

Moreover, let us assume $\dot{\epsilon}_1 = \dot{\epsilon}_t$, $\dot{\epsilon}_2 = \dot{\epsilon}_r$ and $\dot{\epsilon}_3 = \dot{\epsilon}_z$. Then we find the principal strain rates under steady state conditions as follows:

$$\begin{aligned}\dot{\epsilon}_t &= \frac{\dot{w}}{r} = k \sigma_t^n \left[1 - \frac{\sigma_r}{2\sigma_t} \right] f(t) g(T) \\ \dot{\epsilon}_r &= \frac{dw}{dr} = k \sigma_t^n \left[\frac{\sigma_r}{\sigma_t} - \frac{1}{2} \right] f(t) g(T) \\ \dot{\epsilon}_z &= - (\dot{\epsilon}_t + \dot{\epsilon}_r)\end{aligned}\tag{10}$$

Case I. Constant Thickness and Constant Temperature

Hollow Disk Under Steady-State Conditions

Now we consider a constant thickness disk, Figure 3, of outside radius r_0 and inside radius r_1 subjected to a constant temperature under steady-state conditions.

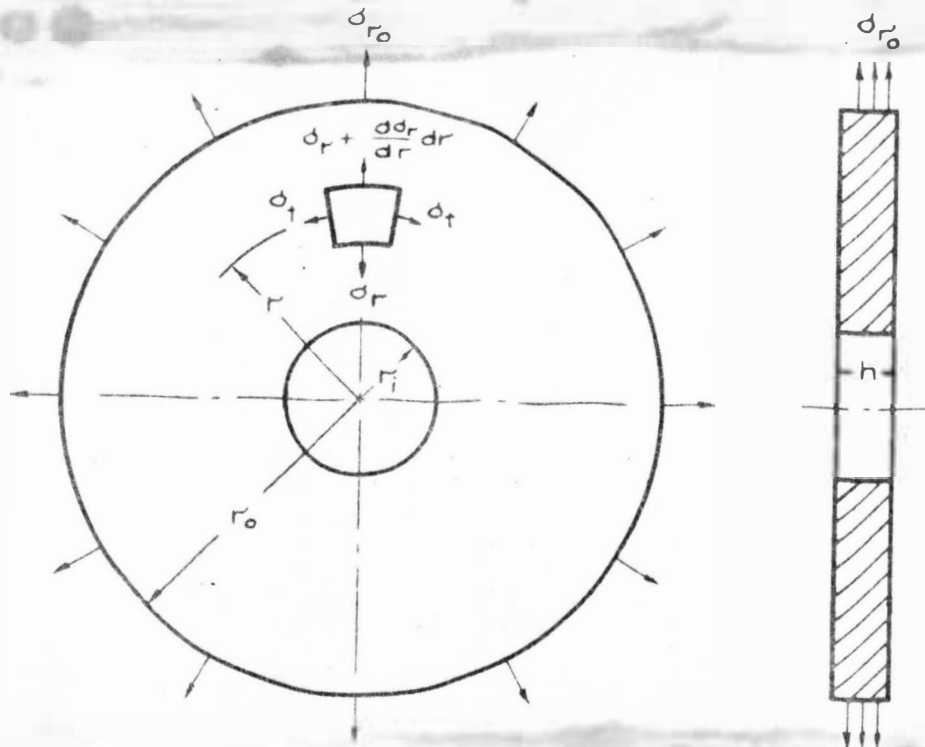


Figure 3. Constant - Thickness Rotating Hollow Disk

By employing the maximum shear theory or the Tresca criterion, Equations (10) can be written as follows:

$$\begin{aligned}
 \dot{\epsilon}_t &= \frac{\dot{w}}{r} = k \sigma_t^n \left(1 - \frac{x}{2}\right) f(t) g(T) \\
 \dot{\epsilon}_r &= \frac{d\dot{w}}{dr} = k \sigma_t^n \left(x - \frac{1}{2}\right) f(t) g(T) \\
 \dot{\epsilon}_z &= -(\dot{\epsilon}_t + \dot{\epsilon}_r)
 \end{aligned} \tag{11}$$

Where the stress ratio $x = \sigma_r / \sigma_t$

From the first two of Equations (11), we may form a function

$\phi(r)$ which is expressed in terms of the stress ratio x . That is

$$\phi(r) = \frac{\dot{\epsilon}_r}{\dot{\epsilon}_t} = \frac{d\dot{w}}{\dot{w}} \cdot \frac{r}{dr} = \frac{2x-1}{2-x} \quad (12)$$

where x at a particular point is approximately known from the stresses already determined. This equation may be rearranged, thus one has

$$\frac{d\dot{w}}{\dot{w}} = \frac{\phi(r)}{r} dr$$

which, after integrating between r_1 and r and then dividing both sides of the equation by r , gives

$$\frac{\dot{w}}{r} = \frac{\dot{w}_1}{r_1} e^{\int_{r_1}^r \frac{\phi(r)}{r} dr} \quad (13)$$

where \dot{w}_1 is the radial deformation rate at radius r_1 .

Using the first of Equations (11) and Equation (13), and solving for $\dot{\sigma}_t$, one finds

$$\dot{\sigma}_t = \left[\frac{\dot{w}_1}{k f(t) g(T)} \right]^{\frac{1}{n}} \psi(r) \quad (14)$$

where

$$\psi(r) = \left[\frac{e^{\int_{r_1}^r \frac{\phi(r)}{r} dr}}{r \left(1 - \frac{x}{2}\right)} \right]^{\frac{1}{n}} \quad (15)$$

For a rotating disk of constant thickness, it can be shown¹⁴

¹⁴S. Timoshenko and J. N. Goodier, Theory of Elasticity, Engineering Societies Monographs, pp. 69-73, McGraw-Hill: New York, 1951.

that the equation of equilibrium for an element is given by

$$\frac{d}{dr} (r \sigma_r) - \sigma_t + \rho w^2 r^2 = 0 \quad (16)$$

which must hold whether stresses are elastic or plastic.

Now integrating Equation (16) between the r_1 and r_0 , one obtains

$$\int_{r_1}^{r_0} \sigma_t dr = \frac{\rho w^2}{3} (r_0^3 - r_1^3) + r_0 \sigma_{r_0} - r_1 \sigma_{r_1} \quad (17)$$

in which σ_{r_0} and σ_{r_1} are the radial stresses at radii r_0 and r_1 , respectively.

Then, substituting the value of σ_t obtained by Equation (14) into Equation (17), one has

$$\left[\frac{w_1}{k f(t) g(r)} \right]^{\frac{1}{n}} = \left[r_0 \sigma_{r_0} - r_1 \sigma_{r_1} + \frac{\rho w^2}{3} (r_0^3 - r_1^3) \right] / \int_{r_1}^{r_0} \psi(r) dr \quad (18)$$

which can be used in Equation (14) to give the following equation

$$\sigma_t = \frac{\left[r_0 \sigma_{r_0} - r_1 \sigma_{r_1} + \frac{\rho w^2}{3} (r_0^3 - r_1^3) \right]}{\int_{r_1}^{r_0} \psi(r) dr} \psi(r) \quad (19)$$

Integrating Equation (16) between the limits r_1 and r , thus

$$\sigma_r = \frac{1}{r} \left[\int_{r_1}^r \sigma_t dr - \frac{\rho w^2}{3} (r^3 - r_1^3) + r_1 \sigma_{r_1} \right] \quad (20)$$

Both Equations (19) and (20) are the general expressions for the stress components of the rotating disk with constant thickness.

Supposing that the boundary conditions of the rotating disk are taken into consideration, these are the cases:

Case (1): $\sigma_{r_1} = 0$ and $\sigma_{r_0} \neq 0$

Since a load giving a stress σ_{r_0} acts at the outside radius of the disk, while no load acts on the inside radius of the disk, Equation (19) becomes

$$\sigma_t = \frac{[(r_0 - r_1) \sigma_{tav}]}{\int_{r_1}^{r_0} \psi(r) dr} \psi(r) \quad (21)$$

in which σ_{tav} is the average tangential stress or the first approximation for tangential stress, i.e. $(\sigma_t)_1$, over the cross section of the disk.

$$\sigma_{tav} = \frac{1}{(r_0 - r_1)} \left[\frac{\rho \omega^2}{3} (r_0^3 - r_1^3) + r_0 \sigma_{r_0} \right] \quad (22)$$

and Equation (20) furnishes

$$\sigma_r = \frac{1}{r} \left[\int_{r_1}^r \sigma_t dr - \frac{\rho \omega^2}{3} (r^3 - r_1^3) \right] \quad (23)$$

In order to find the first approximation for the stress ratio (x), for use in Equations (12), (15), and (21) we assume $\sigma_t = \sigma_{tav}$ in Equation (23) and integrate. This gives the first approximation for the radial stress $(\sigma_r)_1$. Then

$$(x)_1 = \frac{(\sigma_r)_1}{\sigma_{tav}} = \frac{1}{r} \left[(r - r_1) - \frac{\rho w^2 (r^3 - r_1^3) (r_0 - r_1)}{\rho w^2 (r_0^3 - r_1^3) + 3r_0 \sigma_{r_0}} \right] \quad (24)$$

Case (ii): $\sigma_{r_1} \neq 0$ and $\sigma_{r_0} = 0$

Since there is a stress σ_{r_1} acting at the inside radius of the disk, while no force acting on the outside radius of the disk, Equation (19) becomes again

$$\sigma_t = \frac{[(r_0 - r_1) \sigma_{tav}]}{\int_{r_1}^{r_0} r \, dr} \quad (21)$$

In this σ_{tav} is the average tangential stress over the cross section

$$\sigma_{tav} = \frac{1}{(r_0 - r_1)} \left[\frac{\rho w^2}{3} (r_0^3 - r_1^3) - r_1 \sigma_{r_1} \right] \quad (25)$$

and Equation (20) remains

$$\sigma_r = \frac{1}{r} \left[\int_{r_1}^r \sigma_t \, dr - \frac{\rho w^2}{3} (r^3 - r_1^3) + r_1 \sigma_{r_1} \right] \quad (20)$$

In order to find the first approximation for the stress ratio $(x)_1$ for use in Equation (12), (15), and (21) we assume $\sigma_t = \sigma_{tav}$ in Equation (20) and integrate. This gives the first approximation for the radial stress $(\sigma_r)_1$. Then

$$(x)_1 = \frac{(\sigma_r)_1}{\sigma_{tav}} = \frac{1}{r} \left\{ (r-r_1) - \frac{\left[\frac{\rho w^2}{3}(r^3-r_1^3) - r_1 \sigma_{r_1} \right] (r_0-r_1)}{\frac{\rho w^2}{3}(r_0^3-r_1^3) - r_1 \sigma_{r_1}} \right\} \quad (26)$$

Case (iii): $\sigma_{r_1} = 0$ and $\sigma_{r_0} = 0$

Since there are no forces acting at the inside and the outside radii of the disk, Equation (19) becomes again

$$\sigma_t = \frac{[(r_0 - r_1) \sigma_{tav}]}{\int_{r_1}^{r_0} r(r) dr} \quad r(r) \quad (21)$$

In this σ_{tav} is the average tangential stress over the cross section

$$\sigma_{tav} = \frac{1}{r_0 - r_1} \left[\frac{\rho w^2}{3} (r_0^3 - r_1^3) \right] \quad (27)$$

and Equation (20) furnishes again

$$\sigma_r = \frac{1}{r} \left[\int_{r_1}^r \sigma_t dr - \frac{\rho w^2}{3} (r^3 - r_1^3) \right] \quad (23)$$

In order to find the first approximation for the stress ratio $(x)_1$ for use in Equation (12), (15), and (21) we assume $\sigma_t = \sigma_{tav}$ in Equation (23) and integrate. This gives the first approximation for the radial stress $(\sigma_r)_1$. Then

$$(x)_1 = \frac{(\sigma_r)_1}{\sigma_{tav}} = \frac{1}{r} \left[(r - r_1) - \frac{(r^3 - r_1^3)(r_0 - r_1)}{(r_0^3 - r_1^3)} \right] \quad (28)$$

With stress distribution known, the creep deformations at steady state conditions may be obtained by integrating Equations (11). Thus, one has

$$\begin{aligned} \epsilon_t &= k \sigma_t^n \left(1 - \frac{x}{2}\right) \int_0^t g(T) f(t) dt \\ \epsilon_r &= k \sigma_t^n \left(x - \frac{1}{2}\right) \int_0^t g(T) f(t) dt \\ \epsilon_z &= -(\epsilon_t + \epsilon_r) \end{aligned} \quad (29)$$

For Case (1):

If we take σ_{t_1} and ϵ_{t_1} to be the stress and creep deformation at the inside radius of the disk at time t_1 , then

$$\epsilon_{t_1} = k \sigma_{t_1}^n \int_0^{t_1} g(T) f(t) dt$$

and we can write for the creep deformations at any radius r and time t

$$\begin{aligned} \epsilon_t &= \epsilon_{t_1} \left(\frac{\sigma_t}{\sigma_{t_1}}\right)^n \left(1 - \frac{x}{2}\right) \\ \epsilon_r &= \epsilon_{t_1} \left(\frac{\sigma_t}{\sigma_{t_1}}\right)^n \left(x - \frac{1}{2}\right) \\ \epsilon_z &= -(\epsilon_t + \epsilon_r) \end{aligned} \quad (30)$$

For Case (ii):

If we take σ_{t_0} and ϵ_{t_0} to be the stress and creep deformation at the outside radius of the disk at time t , then

$$\epsilon_{t_0} = k \sigma_{t_0}^n \int_0^t g(T) f(t) dt$$

and we can write for the creep deformations at any radius r and time t

$$\begin{aligned} \epsilon_t &= \epsilon_{t_0} \left(\frac{\sigma_t}{\sigma_{t_0}} \right)^n \left(1 - \frac{x}{2} \right) \\ \epsilon_r &= \epsilon_{t_0} \left(\frac{\sigma_t}{\sigma_{t_0}} \right)^n \left(x - \frac{1}{2} \right) \end{aligned} \quad (31)$$

$$\epsilon_z = -(\epsilon_t + \epsilon_r)$$

For Case (iii):

Either Equation (30) or (31) can be used to calculate the creep deformations of the disk.

Case II. Variable Thickness and Constant Temperature

Hollow Disk Under Steady-State Conditions

We consider a variable thickness disk, Figure 4, of outside radius r_0 and inside radius r_1 subjected to a constant temperature under steady state conditions based on the maximum-shear theory.

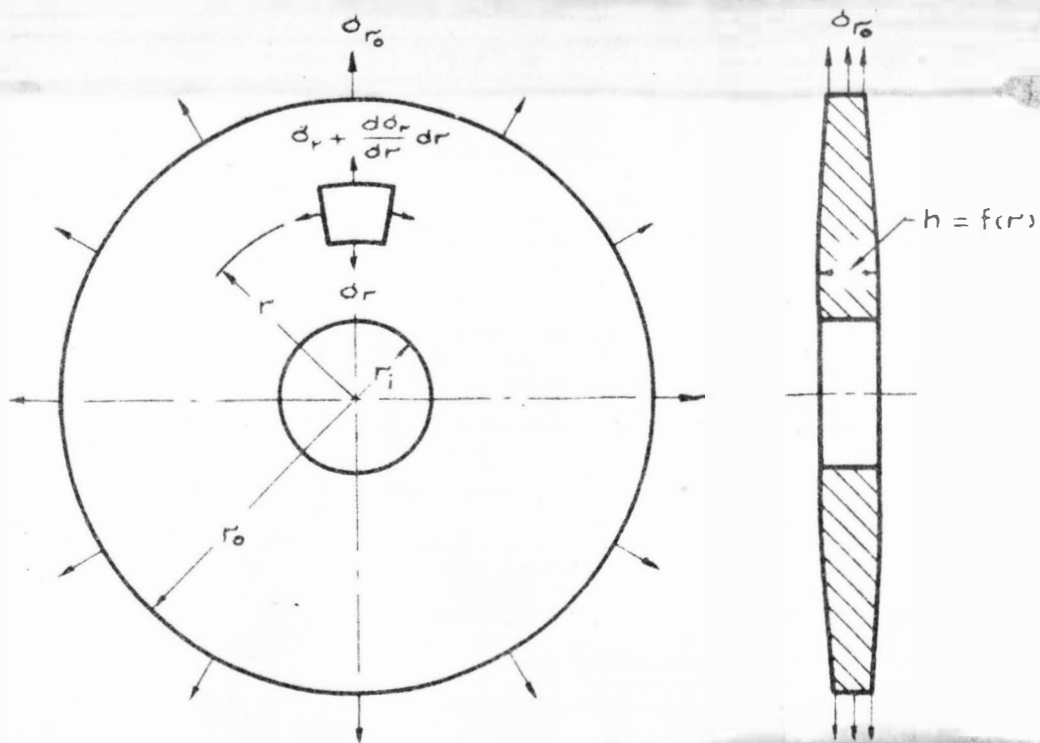


Figure 4. Variable - Thickness Rotating Hollow Disk

Let the disk thickness h be a function of r

$$h = f(r) \quad (32)$$

The known equilibrium equation for a variable thickness disk is

$$\frac{d}{dr} (hr \sigma_r) - h \sigma_t + h \rho \omega^2 r^2 = 0 \quad (33)$$

Now, integrating Equation (33) between the r_i and r_o , one has

$$\int_{r_1}^{r_0} h \delta_t dr = \rho \omega^2 \int_{r_1}^{r_0} hr^2 dr + h_0 r_0 \delta_{r_0} - h_1 r_1 \delta_{r_1} \quad (34)$$

where h_0 and h_1 are the thicknesses at the outside and the inside radii of the disk respectively.

Then, substituting the value of δ_t from Equation (14) into Equation (34), one obtains

$$\left[\frac{w_i}{k f(t)} \right]^{\frac{1}{n}} = \left[\rho \omega^2 \int_{r_1}^{r_0} hr^2 dr + h_0 r_0 \delta_{r_0} - h_1 r_1 \delta_{r_1} \right] / \int_{r_1}^{r_0} h \psi(r) dr \quad (35)$$

which can be used in Equation (14). It gives the following equation

$$\delta_t = \frac{\left[\rho \omega^2 \int_{r_1}^{r_0} hr^2 dr + h_0 r_0 \delta_{r_0} - h_1 r_1 \delta_{r_1} \right]}{\int_{r_1}^{r_0} h \psi(r) dr} \psi(r) \quad (36)$$

Integrating Equation (33) between the limits r_1 and r , then

$$\delta_r = \frac{1}{hr} \left[\int_{r_1}^r h \delta_t dr - \rho \omega^2 \int_{r_1}^r hr^2 dr + h_1 r_1 \delta_{r_1} \right] \quad (37)$$

Both Equation (36) and (37) are the general expressions for the stresses of the rotating disk with variable thickness.

Now, let δ_{tav} be the average tangential stress across the radial cross sectional area A of the disk, and

$$I = \int_{r_1}^{r_0} hr^2 dr$$

equals the moment of inertia of cross section about the axis of the disk. Then

$$\sigma_{tav} = \frac{1}{A} \int_{r_1}^{r_0} h \sigma_t dr \quad (38)$$

If the boundary conditions of the rotating disk are taken into consideration, three cases may be distinguished as follows:

Case (i): $\sigma_{r_1} = 0$ and $\sigma_{r_0} \neq 0$

Under this boundary condition, Equation (36) becomes

$$\sigma_t = \frac{A \sigma_{tav} \epsilon(r)}{\int_{r_1}^{r_0} h \epsilon(r) dr} \quad (39)$$

where

$$\sigma_{tav} = \frac{1}{A} \left[\rho \omega^2 I + h_0 r_0^2 \sigma_{r_0} \right] \quad (40)$$

and Equation (37) furnishes

$$\sigma_r = \frac{1}{hr} \left[\int_{r_1}^r h \sigma_t dr - \rho \omega^2 I_r \right] \quad (41)$$

where

$$I_r = \int_{r_1}^r hr^2 dr$$

equals the moment of inertia of the cross section of the disk up to a radius r , about the axis of the disk.

In order to find the first approximation for the stress ratio $(x)_1$ for use in Equations (12), (15), and (39) we assume $\sigma_t = \sigma_{tav}$ in

Equation (41) and integrate. This gives the first approximation for the radial stress $(\sigma_r)_1$. Then

$$(\sigma_r)_1 = \frac{(\sigma_{rav})_1}{\sigma_{rav}} = \frac{1}{hr} \left[A_r - \frac{\rho w^2 I_r A}{\rho w^2 I + h_0 r_0 \sigma_{r_0}} \right] \quad (42)$$

in which

$$A_r = \int_{r_1}^r h dr$$

This equals the radial cross-sectional area of the disk from the radius r_1 to r .

Case (ii): $\sigma_{r_1} \neq 0$ and $\sigma_{r_0} = 0$

Under this boundary condition, Equation (36) becomes again

$$\sigma_t = \frac{A \sigma_{rav} \psi(r)}{\int_{r_1}^{r_0} h \psi(r) dr} \quad (39)$$

where

$$\sigma_{rav} = \frac{1}{A} \left[\rho w^2 I - h_1 r_1 \sigma_{r_1} \right] \quad (43)$$

and Equation (37) remains

$$\sigma_r = \frac{1}{hr} \left[\int_{r_1}^r h \sigma_t dr - \rho w^2 I_r + h_1 r_1 \sigma_{r_1} \right] \quad (37)$$

In order to find the first approximation for the stress ratio $(\sigma_r)_1$ for use in Equations (12), (15), and (39) we assume $\sigma_t = \sigma_{rav}$ in

Equation (37) and integrate. This gives the first approximation for the radial stress $(\sigma_r)_1$. Then

$$(\sigma_r)_1 = \frac{(\sigma_r)_1}{\sigma_{tav}} = \frac{1}{hr} \left[A_r - \frac{(\rho w^2 I_r - h_1 r_1 \sigma_{r_1}) A}{(\rho w^2 I - h_1 r_1 \sigma_{r_1})} \right] \quad (44)$$

Case (iii): $\sigma_{r_1} = 0$ and $\sigma_{r_0} = 0$

Under this boundary condition, Equation (36) becomes again

$$\sigma_t = \frac{A \sigma_{tav} \psi(r)}{\int_{r_1}^{r_0} h \psi(r) dr} \quad (39)$$

where

$$\sigma_{tav} = \frac{1}{A} [\rho w^2 I] \quad (45)$$

and Equation (37) furnishes again

$$\sigma_r = \frac{1}{hr} \left[\int_{r_1}^r h \sigma_t dr - \rho w^2 I_r \right] \quad (41)$$

In order to find the first approximation for the stress ratio $(\sigma_r)_1$ for use in Equations (12), (15), and (39) we assume $\sigma_t = \sigma_{tav}$ in Equation (41) and integrate. This gives the first approximation for the radial stress $(\sigma_r)_1$. Then

$$(\sigma_r)_1 = \frac{(\sigma_r)_1}{\sigma_{tav}} = \frac{1}{hr} \left[A_r - \frac{I_r A}{I} \right] \quad (46)$$

With stress distribution known, the creep deformations at steady state conditions may be obtained by the very same method used for disks of constant thickness.

NUMERICAL EXAMPLE OF A ROTATING HOLLOW DISK

Let us consider a rotating hollow disk of outside radius $r_0 = 10$ inches, and inside radius $r_1 = 1$ inch at a rotating speed of 12,000 rpm and of variable thickness at constant temperature. The value of the stress exponent n is taken equal to 6. The boundary radial stresses σ_{r_0} and σ_{r_1} are assumed to be negligible. We will determine the stress distribution and relative creep rates in this disk under steady creep conditions.

Before determining the stress distribution and relative deformations in this rotating disk, we may use the same data to calculate the elastic stresses in the disk so that the result will be directly comparable.

Elastic Stresses

Based on the theory of elasticity, the radial and tangential stresses in the case of a rotating hollow disk of variable thickness are given as follows:

$$\sigma_r = \frac{F}{hr} \quad ; \quad \sigma_t = \frac{1}{h} \frac{dF}{dr} + \rho \omega^2 r^2 \quad (a)$$

If the thickness of the disk varies according to the equation

$$h = Cr^m \quad (b)$$

in which C is a constant and m any number, we may find that

$$F = - \frac{(3 + \nu) \rho \omega^2 C}{(\nu m + 3m + 8)} r^{m+3} + C_1 r^\alpha + C_2 r^\beta \quad (c)$$

where α and β are the roots of the quadratic equation

$$x^2 - mx + \nu m - 1 = 0 \quad (d)$$

and C_1 and C_2 are integration constants.

Let $m = -0.5$ and $\nu = 0.3$, then we find, by using Equation (d)

$$\alpha = 0.8512 \text{ and } \beta = -1.3512$$

Since the disk is operated at a speed $N = 12,000$ rpm, then we have

$$\omega = \frac{2\pi}{60} N = 1256.64 \text{ radians/second. Taking } \rho = \frac{0.283}{386} = 0.000733$$

lb-sec²/in⁴ and substituting these values of m , ν , ω , α , and β in Equation (c), we find

$$F = -601.56 C r^{2.5} + C_1 r^{0.8512} + C_2 r^{-1.3512} \quad (e)$$

and the radial stress, from Equation (a) is

$$\sigma_r = \frac{F}{hr} = \frac{1}{Cr^{0.5}} \left[-601.56 Cr^{2.5} + C_1 r^{0.8512} + C_2 r^{-1.3512} \right]$$

Since the boundary stresses are negligible, then we have

$$(\sigma_r)_{r=r_0} = 0, \quad (\sigma_r)_{r=r_1} = 0$$

from which we find that

$$C_1 = 26,961.47C \quad ; \quad C_2 = -26,359.91C$$

Substituting in Equations (a),

$$\delta_r = \frac{1}{r^{0.5}} \left[-601.56 r^{2.5} + 26,961.47 r^{0.8512} - 26,359.91 r^{-1.3512} \right]$$

$$\delta_t = r^{0.5} \left[-1503.90 r^{1.5} + 22,949.60 r^{-0.1488} + 35,617.51 r^{-2.3512} \right] \\ + 1157.51 r^2$$

Calculations for radial and tangential stresses in this disk are carried out in Table I and Table II, respectively, where several values of r are taken, as shown in the first column, and the corresponding stresses are to be found in the last column.

Creep Stresses

Based on the creep analysis which has been presented in this paper, the creep stresses and deformations of this rotating disk can be determined by the method developed in Case (iii) for disks of variable thickness.

From Equation (45), we have

$$\delta_{\text{tav}} = \frac{1}{A} \left[\rho \omega^2 I \right] \quad (a)$$

Since $A = \int_{r_1}^{r_0} h dr$, and $I = \int_{r_1}^{r_0} hr^2 dr$, then we may rewrite Equation (a) as follows:

$$\delta_{\text{tav}} = \frac{1}{\int_{r_1}^{r_0} h dr} \left[\rho \omega^2 \int_{r_1}^{r_0} hr^2 dr \right] \quad (b)$$

TABLE I. CALCULATION OF RADIAL STRESSES IN ROTATING HOLLOW DISK
OF VARIABLE THICKNESS FOR ELASTIC CONDITION

(1)	(2)	(3)	(4)	(5)	(6)	(7)	(8)	(9)
r	$r^{0.5}$	$r^{2.5}$	$r^{0.8512}$	$r^{-1.3512}$	$601.56 \times (3)$	$26961.47 \times (4)$	$26359.91 \times (5)$	$\frac{-(6) + (7) - (8)}{(2)}$
1	1.000	1.000	1.000	1.000	601.56	26961.47	26359.91	0
1.5	1.225	2.756	1.412	0.578	1657.90	38069.60	15236.03	17290
2	1.414	5.656	1.804	0.392	3402.42	48638.49	10333.08	24680
3	1.732	15.588	2.547	0.241	9377.12	68670.86	6352.74	30570
4	2.000	32.000	3.254	0.154	19249.92	87732.62	4059.43	32210
5	2.236	55.900	3.935	0.114	33627.20	106093.38	3005.03	31060
6	2.449	88.164	4.596	0.089	53035.94	123914.92	2346.03	27980
7	2.646	129.654	5.240	0.072	77994.66	141278.10	1897.91	23200
8	2.828	180.992	5.871	0.060	108877.55	158290.79	1581.59	16910
9	3.000	243.000	6.490	0.051	146179.08	174979.94	1344.36	9150
10	3.162	316.200	7.099	0.045	190213.27	191399.47	1186.20	0

TABLE II. CALCULATION OF TANGENTIAL STRESSES IN ROTATING HOLLOW DISK OF VARIABLE THICKNESS FOR ELASTIC CONDITION

	(1)	(2)	(3)	(4)	(5)	(6)	(7)	(8)	(9)	(10)	(11)	(12)	(13)
r	1.000	1.000	1.000	1.000	1.000	1.000	1503.90x(3)	22949.60x(4)	35617.51x(5)	1157.51x(6)	-(-7)+(-8)+(-9)	(2)x(11)	(12)+(10) ρ_c
r_0	1.000	1.000	1.000	1.000	1.000	1.000	1503.90	22949.60	35617.51	1157.51	57063.21	57063.21	58220
r_1	1.225	1.338	0.941	0.3853	2.250	2.250	2764.17	21595.57	13723.43	2604.40	32554.83	32554.83	42460
2	1.414	2.828	0.902	0.1960	4.000	4.000	4253.03	20700.54	6981.03	4630.04	23428.54	23428.54	37760
3	1.732	5.196	0.849	0.0803	9.000	9.000	7814.26	19484.21	2860.09	10417.59	14530.04	14530.04	35380
4	2.000	8.000	0.814	0.0385	16.000	16.000	12031.20	18680.97	1371.27	19520.16	8021.04	16042.08	34580
5	2.236	11.180	0.787	0.0228	25.000	25.000	16813.60	18061.34	812.08	28937.75	2059.82	4605.76	33540
6	2.449	14.694	0.766	0.0148	36.000	36.000	22098.31	17579.39	527.14	41670.36	-3991.78	-9775.87	31890
7	2.646	18.522	0.749	0.0103	49.000	49.000	27855.24	17189.25	366.86	56717.99	-10299.13	-27251.50	29470
8	2.828	22.624	0.734	0.0075	64.000	64.000	34024.23	16845.01	267.13	74080.64	-16912.09	-47827.39	26250
9	3.000	27.000	0.721	0.0057	81.000	81.000	40605.30	16546.66	203.02	93758.31	-23855.62	-71566.66	22190
10	3.162	31.620	0.710	0.0045	100.000	100.000	47553.32	16294.22	160.28	115751.00	-31098.82	-98334.47	17420

Substituting $h = Cr^m$ in Equation (b), we may find that

$$\phi_{\text{tav}} = \rho\omega^2 \frac{m+1}{m+3} \frac{[r_0^{m+3} - r_1^{m+3}]}{[r_0^{m+1} - r_1^{m+1}]} \quad (c)$$

From Equation (46), we have

$$(\phi_r)_1 = \frac{1}{hr} \left[\phi_{\text{tav}} A_r - \phi_{\text{tav}} \frac{I_r^A}{I} \right] \quad (d)$$

Since $A_r = \int_{r_1}^r h dr$, $I_r = \int_{r_1}^r hr^2 dr$ and $\phi_{\text{tav}} = \frac{1}{A} [\rho\omega^2 I]$, then

we may rewrite Equation (d) as follows:

$$(\phi_r)_1 = \frac{1}{hr} \left[\phi_{\text{tav}} \int_{r_1}^r h dr - \rho\omega^2 \int_{r_1}^r hr^2 dr \right] \quad (e)$$

Substituting $h = Cr^m$ in Equation (e), we may find that

$$(\phi_r)_1 = \frac{1}{r^{m+1}} \left[\frac{1}{m+1} (r^{m+1} - r_1^{m+1}) \phi_{\text{tav}} - \frac{1}{m+3} (r^{m+3} - r_1^{m+3}) \rho\omega^2 \right] \quad (f)$$

If the same data used for elastic condition are substituted in Equation (c), then we have

$$\phi_{\text{tav}} = 33760 \text{ psi}$$

and

$$(\sigma_r)_1 = \frac{1}{r^2} \left[67520 (r^{\frac{1}{2}} - 1) - 463,107 (r^{5/2} - 1) \right] \quad (9)$$

Calculation for these stresses $(\sigma_t)_1$ and $(\sigma_r)_1$ are carried out in Table III. With the first approximation of the stress ratios $(x)_1$ known, the $\phi(r)$ can be found by using Equation (12) and is entered in Table IV. Using Equation (15) for $\psi(r)$, the values of $(\sigma_t)_2$ and $(\sigma_r)_2$ may be calculated from Equation (39) and (41) respectively. Thus the second approximation of the stress ratios $(x)_2$ are obtained in the last column of this table. These stresses in the disk are the second approximation of the stresses and are close to the final ones indicated by this method. To obtain a closer solution, another complete cycle of calculations of the stresses was repeated in Table V. Calculations are similar to those of the second approximation. The final values of $(\sigma_t)_3$ and $(\sigma_r)_3$ obtained in Table V are the third approximation of the stresses.

With stress distribution known, the relative creep rates may be calculated by using Equations (30). The tangential creep rate at the inside radius r_1 will be considered as a unity. This differs from the actual creep rates only by a constant which could be easily determined in a practical problem. The results of these calculations are carried out in Table VI.

The results of calculations of elastic and creep stresses are shown in Figure 5 and Figure 6 respectively. For the purposes of

TABLE III. CALCULATION OF FIRST APPROXIMATION FOR STRESSES IN ROTATING HOLLOW DISK OF VARIABLE THICKNESS

(1)	(2)	(3)	(4)	(5)	(6)	(7)	(8)	(9)	(10)	(11)
r	t	$(2) - 1$	$r^{3/2}$	$(4) - 1$	$67520 \times (3)$	$463.107 \times (5)$	$(6) - (7)$	$(\sigma_r)_1$	$(\sigma_r) / (2)$	$(\sigma_r)_1 / (9)$
1	1.000	0	1.000	0	0	0	0	33760	0	0
1.5	1.225	0.225	2.756	1.756	15192	813	14379	33760	11740	0.348
2	1.414	0.414	5.657	4.657	27953	2157	25796	33760	18240	0.540
3	1.732	0.732	15.588	14.588	49425	6756	42669	33760	24640	0.730
4	2.000	1.000	32.000	31.000	67520	14356	53164	33760	26580	0.787
5	2.236	1.236	55.900	54.900	83455	25425	58030	33760	25950	0.769
6	2.449	1.449	88.164	87.164	97836	40366	57470	33760	23470	0.695
7	2.646	1.646	129.644	128.644	111138	59576	51562	33760	19490	0.577
8	2.828	1.828	180.992	179.992	123427	83355	40072	33760	14170	0.420
9	3.000	2.000	243.000	242.000	135040	112070	22970	33760	7660	0.227
10	3.162	2.162	316.228	315.228	145978	145978	0	33760	0	0

TABLE IV. CALCULATION OF SECOND APPROXIMATION FOR STRESSES IN ROTATING HOLLOW DISK OF VARIABLE THICKNESS

(12)	(13)	(14)	(15)	(16)	(17)	(18)	(19)	(20)	(21)	(22)	(23)
$\phi(r)$	$\phi(r)/r$	$\int_{r_1}^r \frac{\phi(r)}{r} dr$	$e \int_{r_1}^r \frac{\phi(r)}{r} dr$	$\psi(r)$	$r^{-\frac{1}{2}} \psi(r)$ (16)/(2)	$\int_{r_1}^{r_0} r^{-\frac{1}{2}} \psi(r) dr$	$39500 \times (18)$ *	(19) - (7)	$39500 \times (16)$ $(\phi_r)_2$	$(\phi_r)_2$ (20)/(2)	$(x)_2^2$ (22)/(21)
-0.500	-0.5000	0	1.000	1.000	1.000	0	0	0	39500	0	0
-0.184	-0.1227	-0.1557	0.856	0.940	0.767	0.442	17459	16646	37200	13600	0.367
0.055	0.0275	-0.1795	0.836	0.911	0.644	0.794	31363	29206	36000	20700	0.575
0.362	0.1207	-0.1054	0.899	0.882	0.509	1.370	54115	47359	34800	27300	0.784
0.473	0.1183	0.0141	1.014	0.865	0.433	1.841	72720	58364	34200	29200	0.854
0.437	0.0874	0.1170	1.124	0.845	0.378	2.247	88757	63332	33400	28300	0.847
0.299	0.0498	0.1856	1.204	0.821	0.335	2.603	102819	62453	32400	25500	0.787
0.108	0.0154	0.2182	1.244	0.793	0.300	2.920	115340	55764	31300	21100	0.674
-0.101	-0.0126	0.2196	1.246	0.763	0.270	3.205	126598	43243	30100	15300	0.508
-0.308	-0.0342	0.1962	1.216	0.731	0.244	3.462	136749	24679	28900	8230	0.285
-0.500	-0.0500	0.1541	1.166	0.699	0.221	3.695	145972	0	27600	0	0
$\Sigma 3.695$											

$$*A \delta_{tav} / \int_{r_1}^{r_0} h \psi(r) dr = 4.324 (33760) / 3.695 = 39500$$

TABLE V. CALCULATION OF THIRD APPROXIMATION FOR STRESSES IN ROTATING HOLLOW DISK OF VARIABLE THICKNESS

(24)	(25)	(26)	(27)	(28)	(29)	(30)	(31)	(32)	(33)	(34)	(35)	
$\phi(r)$	$\phi(r)/z$	$\int_{r_1}^r \frac{\phi(r)}{r} dr$	$e \int_{r_1}^r \frac{\phi(r)}{r} dr$	$\psi(r)$	$r^{-\frac{1}{2}} \psi(r) / (2)$	$\int_{r_1}^{r_0} r^{-\frac{1}{2}} \psi(r) dr$	$37643x(30)$	(31) - (7)	$37643x(28)$	$(\phi_r)^3$	$(\phi_r)^3 / (2)$	$(x)^3$ $(34)/(33)$
-0.500	-0.5000	0	1.000	1.0000	1.000	0	0	0	37600	0	0	0
-0.162	-0.1080	-0.1520	0.859	0.9425	0.769	0.442	16638	15825	35500	12900	0.363	
0.105	0.0525	-0.1659	0.847	0.9169	0.648	0.796	29964	27807	34500	19700	0.571	
0.467	0.1557	-0.0618	0.940	0.8953	0.517	1.479	55674	48918	33700	28200	0.837	
0.618	0.1545	0.0933	1.098	0.8845	0.442	1.958	73705	59349	33300	29700	0.892	
0.602	0.1204	0.2308	1.260	0.8711	0.390	2.374	89364	63932	32800	28600	0.872	
0.473	0.0788	0.3304	1.392	0.8522	0.348	2.743	103255	62890	32100	25700	0.801	
0.262	0.0374	0.3885	1.475	0.8262	0.312	3.073	115677	56103	31100	21200	0.682	
0.011	0.0014	0.4079	1.503	0.7948	0.281	3.370	126857	43504	29900	15400	0.515	
-0.251	-0.0279	0.3946	1.484	0.7595	0.253	3.637	136908	24838	28600	8280	0.290	
-0.500	-0.0500	0.3557	1.427	0.7231	0.229	3.878	145980	0	27200	0	0	
$\Sigma 3.878$												

*A $\phi_{\text{rav}} \int_{r_1}^{r_0} h \psi(r) dr = 4.324 (33760) / 3.878 = 37643$

TABLE VI. CALCULATION OF RELATIVE CREEP RATES BASED ON THE THIRD APPROXIMATION OF THE STRESSES IN ROTATING HOLLOW DISK OF VARIABLE THICKNESS

(1)	(2)	(3)	(4)	(5)	(6)	(7)	(8)
x	$1 - (x)^{3/2}$	$(x)^3 - 1/2$	σ / σ_{th}	$(\sigma_c / \sigma_{t1})^n$ $n = 6$	$\dot{\epsilon}_r / \dot{\epsilon}_{t1} = \dot{\epsilon}_+ / \dot{\epsilon}_{t1}$ (2) x (5)	$\dot{\epsilon}_r / \dot{\epsilon}_{t1} = \dot{\epsilon}_- / \dot{\epsilon}_{t1}$ (3) x (5)	$\dot{\epsilon}_z / \dot{\epsilon}_{t1} = \dot{\epsilon}_z / \dot{\epsilon}_{t1}$
1	1.000	-0.500	1.000	1.0000	1.000	-0.500	-0.500
1.5	0.818	-0.137	0.944	0.7077	0.579	-0.097	-0.482
2	0.714	0.071	0.918	0.5986	0.427	0.045	-0.472
3	0.581	0.337	0.896	0.5174	0.300	0.174	-0.474
4	0.554	0.392	0.886	0.4837	0.268	0.190	-0.458
5	0.564	0.372	0.872	0.4397	0.248	0.164	-0.412
6	0.600	0.301	0.854	0.3879	0.233	0.117	-0.350
7	0.659	0.182	0.827	0.3199	0.211	0.058	-0.269
8	0.742	0.015	0.795	0.2525	0.187	0.004	-0.191
9	0.855	-0.210	0.761	0.1942	0.166	-0.041	-0.125
10	1.000	-0.500	0.723	0.1428	0.143	-0.071	-0.072

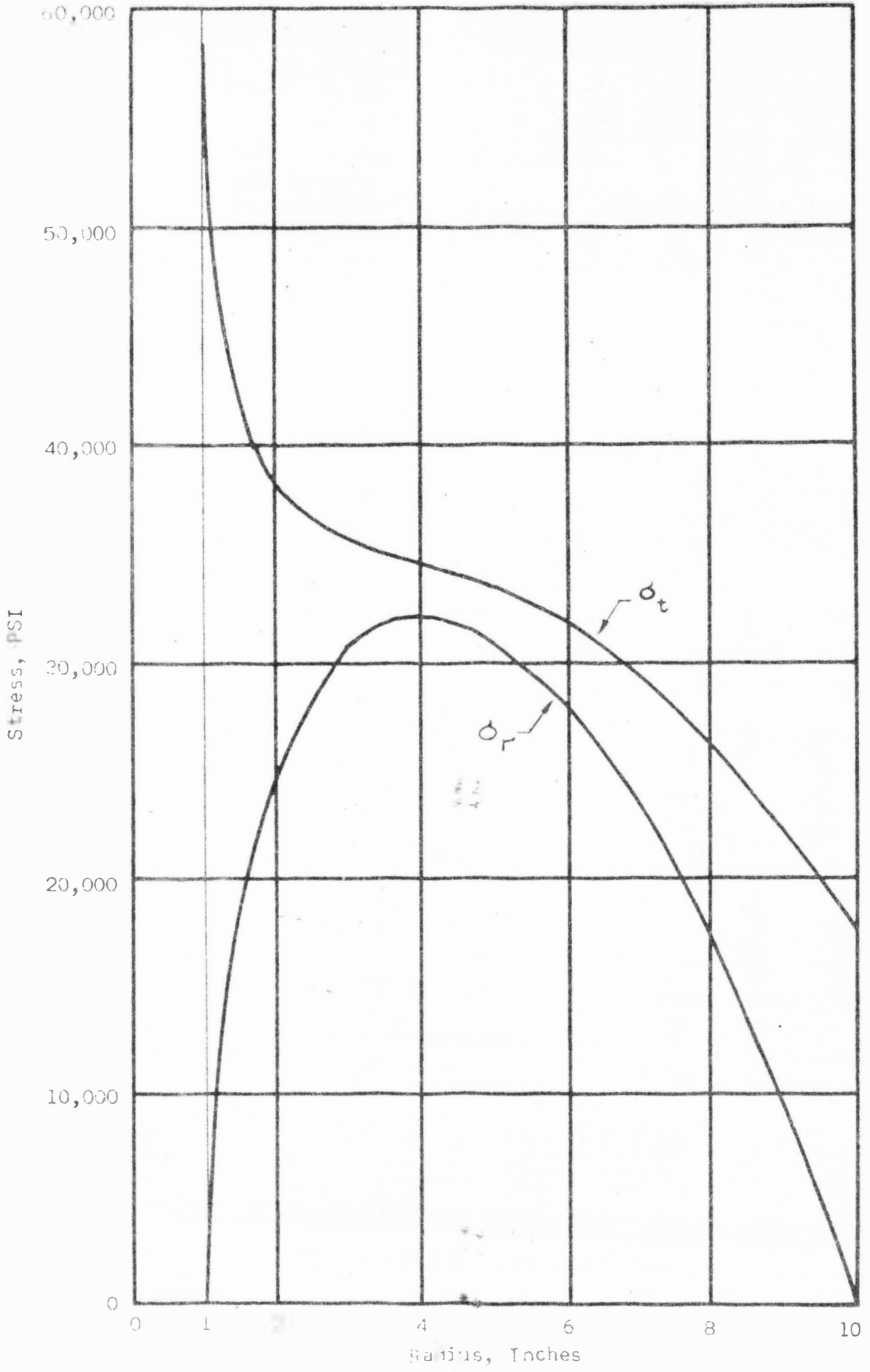


Figure 5. The Stress Distributions of the Disk for Elastic Condition

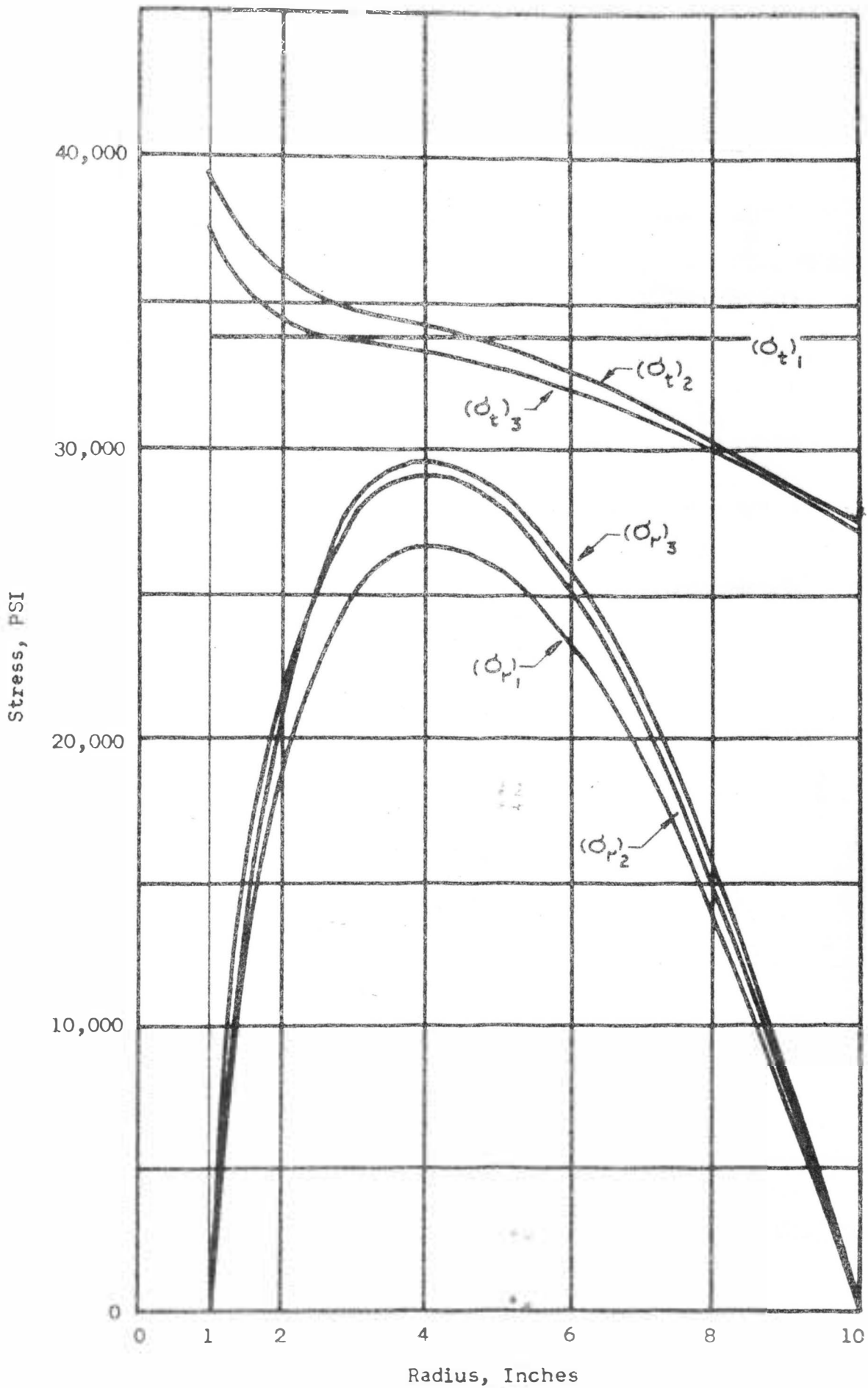


Figure 6. The Stress Distributions of the Disk Under Creep Conditions for $n=6$

comparing the elastic and creep stress distributions, Figure 7 is drawn. It is observed that the successive approximations rapidly approach the desired solution and the steady stress distribution under creep conditions is quite different from that appearing in purely elastic conditions. The maximum tangential stress is approximately 65 percent of the elastic stress and the maximum radial stress is approximately 90 percent for the case considered.

The relative creep rates of this disk calculated by using the third approximation of the stresses are shown in Figure 8.

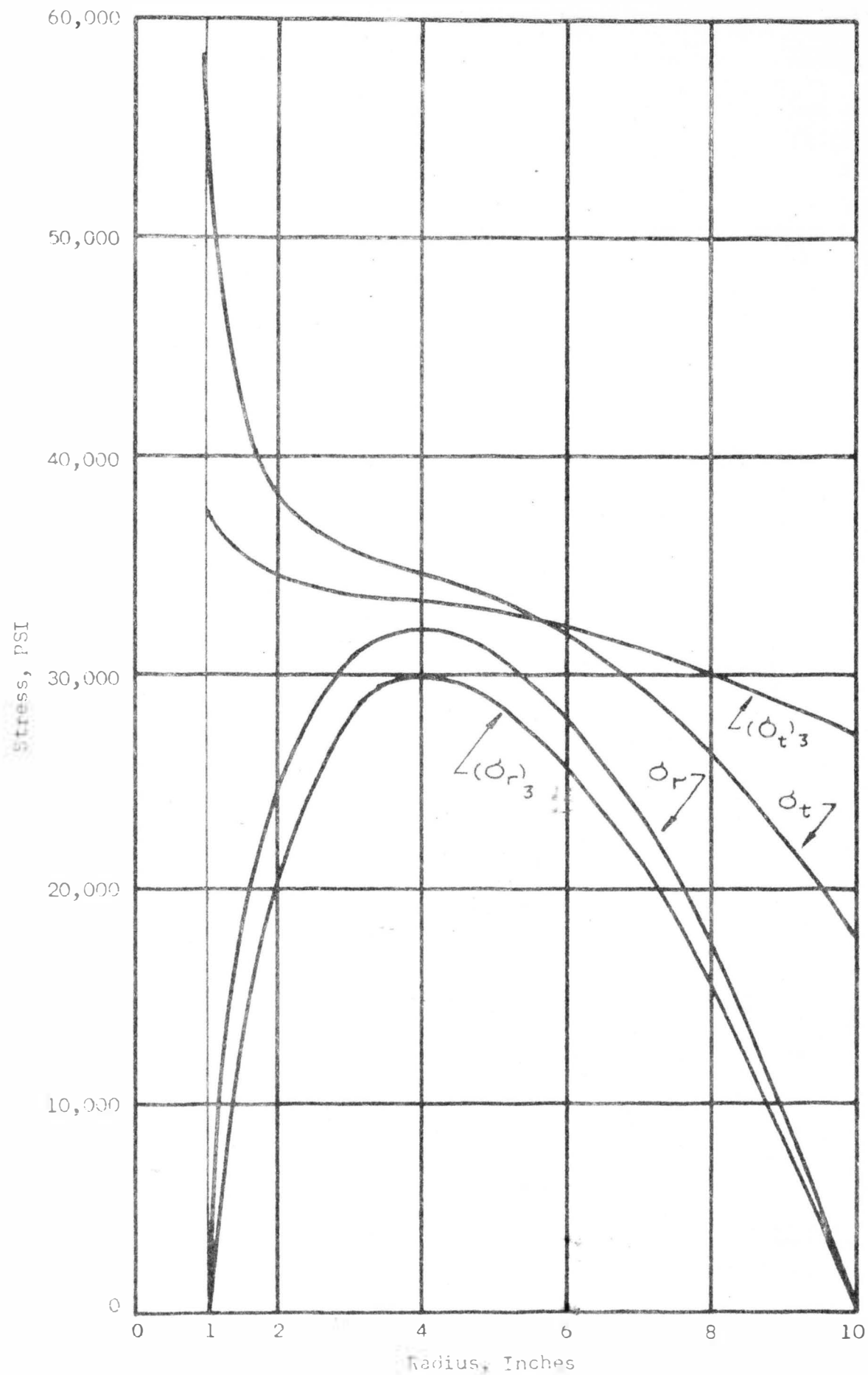


Figure 7. Comparison of Stress Distribution in the Disk Under Elastic and Creep Conditions

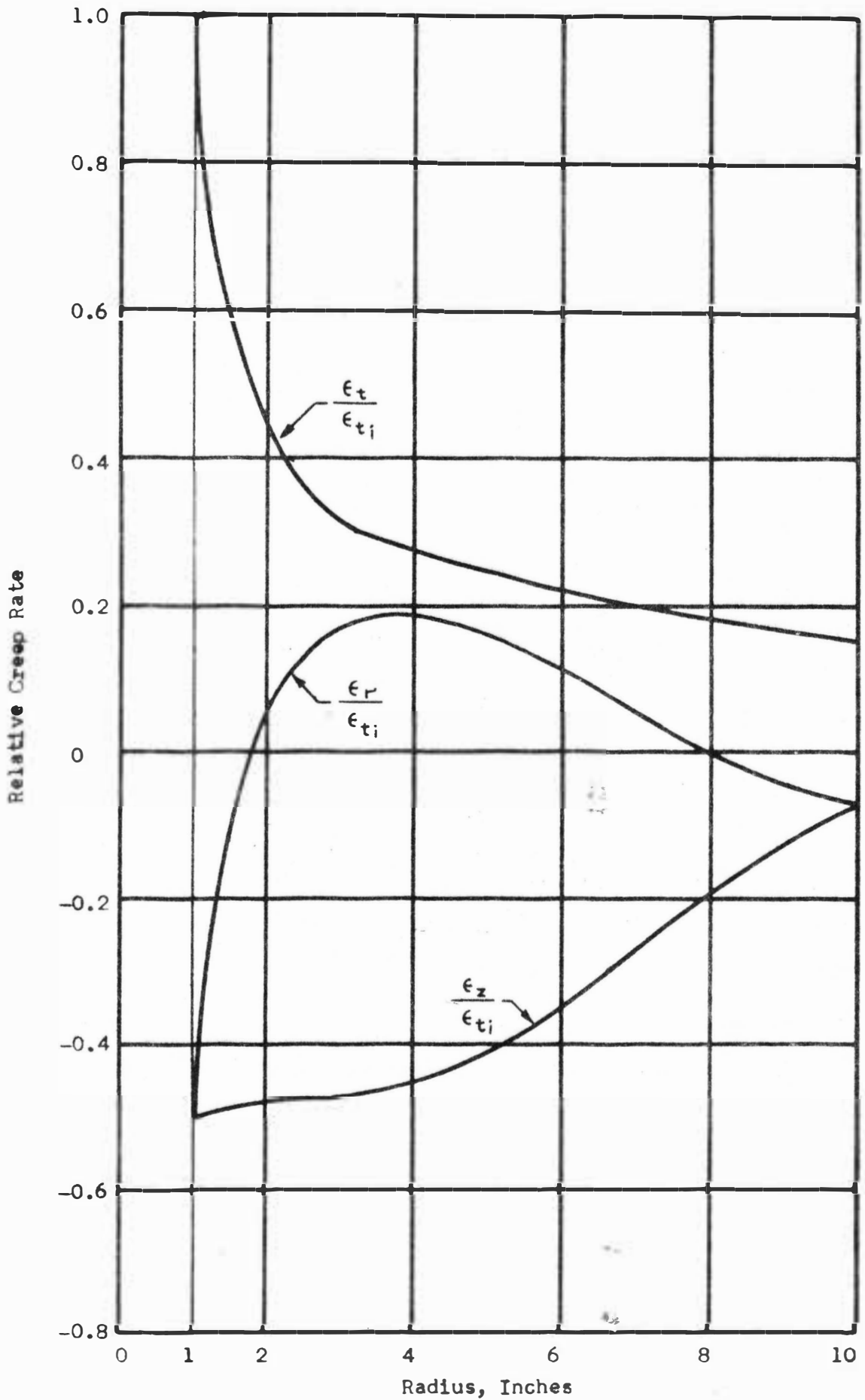


Figure 8. The Relative Creep Rates of the Disk (Based on Third Approximation of the Stresses)

SUMMARY AND CONCLUSIONS

For many years, the problem of creep design has been under active consideration. Analysis of creep problems is usually based on the results available from long-time creep tests. This is the field in which the major efforts have been made by those who are interested in the problem, and a considerable amount of material is available for study. Unfortunately, only a small portion of this material has been accumulated against a background of rational research. Many of the tests were run with a definite purpose from a very limited point of view, so that no attempts were made to bring out clearly the influence of stress, strain, time, and temperature on the creep. These data, nevertheless, are all that we have to work with, and it appears necessary to make more creep test data available.

All long-time creep test results have one feature in common in which the creep deformation proceeds at a very rapid rate at first or primary stage approaching a practically constant rate of deformation at a later stage and then the creep rate gradually increases until fracture takes place (see Figure 2). There has been a general tendency to ignore the initial period of rapid creep rate and to treat the problem as one of constant creep rate. It is evident that this procedure may not be satisfactory for all cases where the stresses are influenced by the plastic deformations. This is nearly always the case in practical problems.

In the problems which are discussed in this paper, the effect of

temperature on creep rate has been left out. In many practical cases, the temperature of the disk may increase from the outside radius toward the center. This means that for the same stress, the creep rate shall increase with increase in radius. In order to take the effect of such temperature variations on the stress distribution in the disk into consideration, the temperature in the creep rate-stress-time-temperature relation for a given material can be no longer treated as a constant and may be further expressed as a function of the radius of the disk.

Recent experimental investigations on the effect of high stress on the creep rate at elevated temperature on pure aluminum and its alloys¹⁵ revealed that the power function stress-creep-rate relation is valid for metals only at relatively low stresses, it does not fit over the high stress range. It is, therefore, suggested that the exponential stress-creep-rate relation may be substituted when the analysis of creep deformation is carried out at high stresses.

The method of analysis of creep deformation in rotating disks presented in this paper is based on the maximum shear theory also known as Tresca interior and the flow rule associated with Mises

¹⁵H. Laks, C. D. Wiseman, O. D. Sherby, and J. E. Dorn, "Effect of Stress on Creep at High Temperatures," Journal of Applied Mechanics, vol. 24, No. 2, pp. 207-213, The American Society of Mechanical Engineers: New York, June, 1957.

criterion in plasticity theory. In view of Drucker's¹⁶ strong theoretical arguments against the application of a flow rule other than the one properly associated with the yield condition, it would be more likely in the purely mathematical basis to use the theory of plasticity based on the Tresca's yield condition and its associated flow rule, rather than to combine a yield condition with an often used flow rule. At present, however, the method which has been presented in this paper appears to give the best over-all agreement with available test results¹⁷ and therefore it may be used as a guide to determine the creep stresses in design problems.

Although some progress has been made during recent years in developing some of the basic laws for creep at high temperature, yet much remains to be done in order to achieve a complete understanding of the phenomenon of creep. The proof of the existence of a steady state is of great importance, however, not only because it will make the tedious calculation unnecessary, but also because it permits a more exact determination of the stresses which eventually will be reached.

¹⁶D. C. Drucker, "A More Fundamental Approach to Plastic Stress-Strain Relations," Proc. The First National Congress of Applied Mechanics, Chicago, 1951, pp. 487-491, J. W. Edwards: Ann Arbor, Michigan, 1952.

¹⁷A. M. Wahl, "Analysis of Creep in Rotating Disks Based on the Tresca Criterion and Associated Flow Rule," Journal of Applied Mechanics, vol. 23, No. 2, pp. 231-238, The American Society of Mechanical Engineers: New York, June, 1956.

LITERATURE CITED

- Bailey, R. W., "The Utilization of Creep Test Data in Engineering Design," Proc. Institution of Mechanical Engineers, vol. 131, 131-349, Institute of Mechanical Engineers: London, November, 1935.
- Bailey, R. W., "Creep Relationships and Their Application to Pipes, Tubes, and Cylindrical Parts Under Internal Pressure," Proc. Institution of Mechanical Engineers, vol. 164, 425, Institute of Mechanical Engineers: London, 1951.
- Drucker, D. C., "A More Fundamental Approach to Plastic Stress-Strain Relations," Proc. The First National Congress of Applied Mechanics, Chicago, 1951, pp. 487-491, J. W. Edwards: Ann Arbor, Michigan, 1952.
- Johnson, A. E., "Creep Under Complex Stress Systems at Elevated Temperatures," Proc. Institution of Mechanical Engineers, vol. 164, 433, Institute of Mechanical Engineers: London, 1951.
- Johnson, A. E., "Turbine Disks for Jet Propulsion Units," Aircraft Engineering, pp. 265-272, Aircraft Engineering: England, August, 1956.
- Laks, H., Wiseman, C. D., Sherby, O. D., and Dorn, J. E., "Effect of Stress on Creep at High Temperatures," Journal of Applied Mechanics, vol. 24, No. 2, pp. 207-213, The American Society of Mechanical Engineers: New York, June, 1957.
- Millenson, M. B., and Manson, S. S., "Determination of Stresses in Gas-Turbine Disks Subjected to Plastic Flow and Creep," NACA Report No. 906, National Advisory Committee for Aeronautics: Washington, D. C., 1948.
- Nadai, A., Plasticity, Engineering Societies Monographs, McGraw-Hill: New York, 1931.
- Nadai, A., Theory of Flow and Fracture of Solids, Monographs, pp. 231-237, McGraw-Hill: New York, 1950.
- Odquist, F. K. G., "Recent Advances in Theories of Creep of Engineering Materials," Applied Mechanics Reviews, vol. 7, 517, The American Society of Mechanical Engineers: New York, 1954.

- Popov, E. P., "Stresses in Turbin Disks at High Temperatures," Journal of the Franklin Institute, vol. 243, 365-389, Franklin Institute: Philadelphia, Pennsylvania, 1947.
- Sherby, O. D., and Dorn, J. E., "An Analysis of the Phenomenon of High Temperature Creep," Proc. Society for Experimental Stress Analysis, vol. XII, No. 1, pp. 139-153, Society for Experimental Stress Analysis: Cambridge, Massachusetts, 1954.
- Soderberg, C. R., "The Interpretation of Creep Tests for Machine Design," Trans. ASME, vol. 58, 733-743, The American Society of Mechanical Engineers: New York, 1936.
- Timoshenko, S., and Goodier, J. N., Theory of Elasticity, Engineering Societies Monographs, pp. 69-73, McGraw-Hill: New York, 1951.
- Wahl, A. M., "Analysis of Creep in Rotating Disks Based on the Tresca Criterion and Associated Flow Rule," Journal of Applied Mechanics, vol. 23, No. 2, pp. 231-238, The American Society of Mechanical Engineers: New York, June, 1956.
- Wahl, A. M., Sankey, G. O., Manjoine, M. J., and Shoemaker, E., "Creep Tests of Rotating Disks at Elevated Temperature and Comparison with Theory," Trans. ASME, vol. 76, 225-235, The American Society of Mechanical Engineers: New York, 1954.